Supporting Information

Singh et al. 10.1073/pnas.1321621111

SI Materials and Methods

Expression and Purification of GsPutA. The gene encoding proline utilization A (PutA) from *Geobacter sulfurreducens* PCA (GsPutA) (1,004 residues; National Center for Biotechnology Information RefSeq number NP_954435.1) in plasmid pNIC28-Bsa4 was obtained from the New York Structural Genomics Research Consortium. The expressed protein includes an N-terminal His tag that is cleavable with Tobacco Etch Virus protease (TEVP).

The GsPutA construct was transformed into BL21AI cells and plated onto LB Agar supplemented with 40 μg/mL kanamycin. A single colony of the transformant was picked to inoculate a 10-mL starter culture containing 1% tryptone and 0.5% yeast extract. The starter culture was incubated at 37 °C overnight with constant shaking at 250 rpm. The next day, this starter culture was used to inoculate 1 L of autoinduction culture. The inoculated culture was incubated at 37 °C for 2 h with shaking at 250 rpm. Next, the temperature of the shaker was reduced to 18 °C, and 0.2% arabinose was added to the media. The cells were harvested after 24 h by centrifugation at 3,500 rpm and 4 °C. The resulting pellet was resuspended in buffer A [20 mM Tris, 150 mM NaCl, and 10% (vol/vol) glycerol at pH 7.5]. The suspension was flash-frozen in liquid N_2 and stored at −80 °C for further use.

Frozen GsPutA cells were thawed at 4 °C in the presence of 1 mM PMSF for 15–20 min with stirring and then disrupted using sonication. Unbroken cells and debris were removed by centrifugation at 4 °C for 60 min at 16,500 rpm in a Sorvall SS-34 fixed angle rotor. The supernatant was transferred into fresh tubes, and the centrifugation step was repeated for 30–45 min. The resulting supernatant was loaded onto an immobilized metal-ion affinity chromatography column (Ni^{2+}-charged HisTRAP; GE Healthcare). The protein was eluted using buffer A supplemented with 1 M imidazole. The fractions containing GsPutA were pooled and mixed with TEVP (1 mg of TEVP per 40 mg of GsPutA) and 1mM Tris(3-hydroxypropyl)phosphine (THP). The sample was incubated at 20 °C for 7 h and dialyzed against buffer A. The dialyzed protein was loaded onto the Ni^{2+}-charged HisTRAP column, and tag-free GsPutA fractions were collected in the flow-through. Purified GsPutA was dialyzed into 10 mM Tris, 25 mM NaCl, 1 mM EDTA, and 1 mM THP at pH 7.5.

Crystallization of Oxidized GsPutA. Initial crystallization conditions were identified using commercially available crystal screening kits (Hampton Research). All trials were performed at room temperature using GsPutA at a concentration of 6 mg/mL as estimated by the Bradford method. Sitting drop, hanging drop, and microbatch methods were used. Drops were formed by combining equal volumes of the protein and reservoir solutions (typically 1–2 μL of each). When using the microbatch method, 1.4 μL of the protein solution was covered with 10 μL of Al's oil (Hampton Research), and 1.4 μL of the precipitant was added to the protein by pipetting through the oil layer.

Three crystal forms of the oxidized enzyme were used in this study. Form 1 was used for preparation of a heavy-atom derivative for phasing and to determine the structure of GsPutA complexed with a detergent molecule. Form 2 crystals were more reproducible than form 1 and were used for crystal-soaking experiments. Form 3 is similar to form 2 but has an adventitious L-lactate ion, which is a competitive inhibitor of proline dehydrogenases (PRODHs), bound in the PRODH active site.

Crystal form 1 was obtained when GsPutA (6 mg/mL) was incubated with 4 mM Zwittergent 3-12 before crystallization. Crystal screening using the microbatch method identified a promising hit in Hampton Index reagent 86, which contains potassium sodium tartrate and PEG 3350. Optimization of this condition yielded diffraction quality crystals with 0.10–0.25 M potassium sodium tartrate and 20–25% (wt/vol) PEG 3350. The crystals were cryoprotected using 28% (wt/vol) PEG 3350, 0.10 M potassium sodium tartrate, and 25% (vol/vol) ethylene glycol. The cryoprotected crystals were picked up with Hampton loops and flash cooled in liquid nitrogen. The space group is $P2_12_12_1$ with a = 94 Å, b = 157 Å, and c = 191 Å. The asymmetric unit includes one GsPutA dimer and 61% solvent (V_M = 3.1 Å^3/Da). The PRODH site of one protomer has an L-lactate ion bound in the proline site. We note that L-lactate is a known inhibitor of PRODH (1) and a contaminant in some commercially available PEGs (2). Thus, the L-lactate bound to the enzyme in the crystal structure likely derives from the PEG 3350 that was used in crystallization and cryoprotection.

Crystal form 2 was obtained when GsPutA was incubated with either 0.1% n-octyl β-D-glucopyranoside (BOG) or 6 mM CHAPS before crystallization. Crystal screening in microbatch plates yielded initial crystals grown in the presence of PEG 550 MME, Bis-Tris buffer at pH 6.5, and $CaCl_2$. Upon optimization, crystals appeared within 1 d and grew to full size within 3 d. The optimized crystallization condition consists of 25–28% (vol/vol) PEG 550 MME, 0.05–0.15 M Bis-Tris at pH 6.3–6.5, and 0.05 M $CaCl_2$. The crystals were cryoprotected in 30% (vol/vol) PEG 550 MME, 0.1 M Bis-Tris (pH 6.5), 0.05 M $CaCl_2$, and 25% (vol/vol) ethylene glycol. The space group is $P2_12_12_1$ with a = 95 Å, b = 151 Å, and c = 175 Å. The asymmetric unit includes one GsPutA dimer and 56% solvent (V_M = 2.8 Å^3/Da). Although forms 1 and 2 have the same space group and similar unit-cell dimensions, they are in fact different crystal forms and exhibit different crystal-packing diagrams. In particular, note that form 1 has a 9% longer c-axis and higher solvent content than form 2. Unlike the other crystal forms described here, the PRODH and Δ^1-pyrroline-5-carboxylate dehydrogenase (P5CDH) substrate sites of form 2 crystals are devoid of bound ligands. Also, these crystals are highly reproducible. For these reasons, crystal form 2 was used for ligand-soaking experiments.

A third crystal form was obtained when detergent was omitted from the setup. Crystal screens performed in sitting drops yielded rod-shaped crystals grown in the presence of PEG 400. Several rounds of streak seeding were done to obtain diffraction-quality crystals. The best crystals were obtained using 21–23.5% (vol/vol) PEG 400 and 0.05–0.2 M 2-(N-morpholino)ethanesulfonic acid (MES) at pH 5.8–6.0. The crystals were cryoprotected using 35–40% (vol/vol) PEG 400 and 0.1 M MES at pH 5.8–6.0. The space group and unit-cell dimensions are identical to those of form 2; however, the PRODH active site of form 3 contains an L-lactate ion bound in the proline site, and the P5CDH active site contains an MES buffer molecule bound in the L-glutamate-γ-semialdehyde (GSA) site. L-lactate is a known inhibitor of PRODH (1) and a contaminant in some commercially available PEGs (2).

Crystal-Soaking Experiments. Crystals of oxidized GsPutA complexed with the proline analog L-tetrahydro-2-furoic acid (THFA) were obtained by soaking form 2 crystals for 10–30 min in the cryobuffer supplemented with 10–50 mM THFA before flash-cooling in liquid nitrogen.

Crystals of GsPutA with the flavin reduced were prepared by soaking form 2 crystals in the cryobuffer supplemented with 0.1 M sodium dithionite. During soaking, the crystals turned from yellow, which is indicative of the oxidized flavin, to colorless, which is

consistent with the two-electron reduced state. After the color transformation was complete (2–5 min), the crystal was harvested with a mounting loop and plunged into liquid nitrogen.

Preparation of a Mercury Derivative for Phasing. Crystal form 1 was used to prepare a mercury derivative. The cryoprotected crystals were transferred to solution containing 28% (wt/vol) PEG 3350, 0.10 M potassium-sodium tartrate, 25% (vol/vol) ethylene glycol, and 0.1 M thimerosal. After soaking for 1–5 min, the crystals were picked up with Hampton loops and flash-frozen in liquid nitrogen.

Crystallization of Inactivated GsPutA. Crystals of GsPutA inactivated by the irreversible inactivator *N*-propargylglycine (NPPG) were grown using the form 2 recipe except that detergent was omitted from the setup. Before crystallization, the enzyme was incubated with NPPG (1 mg of PPG per 1 mg of enzyme). The addition of NPPG caused bleaching of the yellow enzyme solution, which is consistent with reduction of the FAD. Optimized crystals were grown in microbatch trays using 25–33% (vol/vol) PEG 550 MME, 0.05–0.2 M Bis-Tris (pH 6.4–6.5), and 0.05 mM $CaCl_2$. The crystals were cryoprotected using 32% (vol/vol) PEG 550 MME, 0.1 M Bis-Tris (pH 6.5), 0.05 mM $CaCl_2$, and 25% (vol/vol) ethylene glycol.

Crystals of a GsPutA–quinone complex were prepared by cocrystallizing NPPG-inactivated GsPutA with menadione sodium bisulfite (MB). The PEG 550 MME recipe was used except that the crystals were grown in hanging drops rather than microbatch. Before crystallization, GsPutA, inactivated as described in the preceding paragraph, was incubated with 10 mM MB. Crystals were grown in hanging drops using a reservoir of 25–33% (vol/vol) PEG 550 MME, 0.05–0.2 M Bis-Tris (pH 6.4–6.5), and 0.05 mM $CaCl_2$. The crystals were cryoprotected as described in the preceding paragraph except that, immediately before flash cooling, the cryoprotected crystal was soaked for a few seconds in the cryobuffer supplemented with 100 mM MB.

X-Ray Diffraction Data Collection, Phasing, and Refinement. X-ray diffraction data were collected on Advanced Photon Source beamlines 24ID-C/E and Advanced Light Source beamline 4.2.2 (Tables S1–S3). The data were processed with XDS (3) and SCALA (4). The initial structure of GsPutA was determined with single-wavelength anomalous diffraction (SAD) phasing based on a mercury derivative (Table S1). Heavy-atom constellations and initial phases were determined from each mercury dataset using the SHELX C/D/E programs (5) via HKL2MAP (6). These calculations identified a promising 2.57-Å dataset having six Hg sites (Table S1). The sites from SHELX were input to PHENIX AutoSol (7) for SAD phasing, density modification with noncrystallography symmetry averaging, and automated model building. The model thus built was adjusted manually and input to phenix.autobuild for phase extension using higher resolution native dataset (Table S2). The model from automated building was completed with several rounds of model building in COOT (8) and refinement with PHENIX (9). An advanced model was used to initiate refinements of the other GsPutA structures. Structure validation was performed with MolProbity (10) and the PDB (11) validation servers. Refinement statistics are listed in Tables S2 and S3. The Ramachandran plot statistics listed in Tables S2 and S3 were generated with RAMPAGE (12) via the Protein Data Bank (PDB) validation server.

Small-Angle X-Ray Scattering. Small-angle X-ray scattering (SAXS) data were collected on Advanced Light Source beamline 12.3.1 through the mail-in program (13, 14). Before SAXS analysis, GsPutA was subjected to size-exclusion chromatography using a Superdex-200 column equilibrated with 0.05 M Tris (pH 8.0), 0.5 M NaCl, and 1 mM THP. SAXS analysis was performed at three different concentrations (1.1 mg/mL, 1.5 mg/mL, and 2.2 mg/mL). For each protein concentration, scattering intensities were measured using exposure times of 0.5, 1.0, 3.0, and 6.0 s. The scattering curves collected from the protein samples were corrected for background scattering using intensity data collected from the effluent of size-exclusion chromatography. A composite scattering curve for each protein concentration was generated with PRIMUS (15) by scaling and merging the background-corrected high q region from the 3-s exposure with the low q region from the 0.5-s or 1.0-s exposure. PRIMUS was also used for Guinier analysis. Shape-reconstruction calculations were performed with the sastbx.shapeup module of the Small Angle Scattering ToolBox (SASTBX) via the SASTBX server (16). The shape reconstruction calculations used the PISA database of shapes. The FoXS server was used to calculate SAXS profiles from atomic coordinates (17).

Kinetic Measurements. All PRODH kinetic data were collected on a Hi-Tech Scientific SF-61DX2 model stopped-flow spectrometer at 23 °C in 50 mM Hepes, 25 mM NaCl (pH 7.4) using 0.25 μM GsPutA. PRODH activity was measured by following the reduction of menadione (ε = 14,000 $M^{-1}{\cdot}cm^{-1}$) and MB (ε = 8,200 $M^{-1}{\cdot}cm^{-1}$) at 262 and 266 nm, respectively. The K_m and k_{cat} for menadione and MB were determined by varying menadione (2–400 μM) and MB (2.5–200 μM), while holding proline constant at 350 mM. Likewise, K_m and k_{cat} for proline were determined by varying proline (10–950 mM) and holding the menadione and MB concentrations at 100 μM and 150 μM, respectively.

P5CDH activity was measured by following NAD^+ reduction at 340 nm (ε = 6,220 $M^{-1}{\cdot}cm^{-1}$) using a Powerwave XS microplate spectrophotometer (Bio-Tek). P5CDH kinetic parameters were determined using 0.75 μM GsPutA in 50 mM potassium phosphate (pH 7.5, 600 mM NaCl) and varying L-P5C concentration (25–4,000 μM) while holding NAD^+ fixed at 0.2 mM. The effective concentration of L-P5C was estimated based on the equilibrium of P5C/GSA at pH 7.5 as previously reported (18). The K_m and k_{cat} values determined for P5CDH activity are 35 μM L-P5C and 7.5 s^{-1}.

The PRODH and P5CDH coupled reaction of GsPutA was examined by following the production of NADH as previously described (18). Assays were performed in 50 mM potassium phosphate buffer (pH 7.5, 600 mM NaCl) using 40 mM proline, 150 μM menadione, 0.2 mM NAD^+, and 0.75 μM GsPutA. Reduction of NAD^+ was followed (ε_{340} = 6,220 $M^{-1}{\cdot}cm^{-1}$) with a Cary 50 UV-Vis spectrophotometer. Spectral interference of menadione reduction at 340 nm was subtracted from the final progress curves by performing assays in the presence and absence of NAD^+, as described previously (18). A progress curve for two noninteracting PRODH and P5CDH enzymes was simulated using the free diffusion model described by Eq. **S1** (19).

$$[\mathrm{NADH}] = v_1 t + (v_1/v_2)\, K_m \left(e^{-v_2 t/K_m} - 1\right) \qquad \textbf{[S1]}$$

In this equation, v_1 is the rate of PRODH activity under the reaction conditions (2.8 μM·min^{-1}). The parameters v_2 (5.6 μM·min^{-1}) and K_m (35.5 μM) are the steady-state kinetic parameters for P5CDH activity of GsPutA. Comparison of the experimental GsPutA progress curve and the simulated progress curve for noninteracting enzymes is shown in Fig. 3*A*. The overall GsPutA reaction occurs without a perceived lag phase consistent with a channeling mechanism for the coupled PRODH-P5CDH reaction.

Calculations of the Electrostatic Potential. Maps of the electrostatic potential surface were calculated with CCP4mg (20). For these calculations, omitted side chains and loops were modeled with SWISS-MODEL (21) to account for all of the partial charges in the protein. The maps calculated from the modeled structure are not qualitatively different from those calculated from the crystal structure.

Sequence Analysis. The conservation of residues lining the tunnel of GsPutA was determined using sequence alignments calculated with CLUSTALW2 (22) and visualized with ESPript (23). Forty-seven PutA sequences were used. This group has pairwise identities of 15–99% and encompasses the entire PutA phylogenetic tree. This analysis revealed 67 identical residues. The identical residues were then mapped onto the GsPutA structure manually.

1. Zhang M, et al. (2004) Structures of the Escherichia coli PutA proline dehydrogenase domain in complex with competitive inhibitors. *Biochemistry* 43(39):12539–12548.
2. Zhang M, Tanner JJ (2004) Detection of L-lactate in polyethylene glycol solutions confirms the identity of the active-site ligand in a proline dehydrogenase structure. *Acta Crystallogr D Biol Crystallogr* 60(Pt 5):985–986.
3. Kabsch W (2010) XDS. *Acta Crystallogr D Biol Crystallogr* 66(Pt 2):125–132.
4. Evans P (2006) Scaling and assessment of data quality. *Acta Crystallogr D Biol Crystallogr* 62(Pt 1):72–82.
5. Sheldrick GM (2008) A short history of SHELX. *Acta Crystallogr A* 64(Pt 1):112–122.
6. Pape T, Schneider TR (2004) HKL2MAP: A graphical user interface for macromolecular phasing with SHELX programs. *J Appl Cryst* 37(5):843–844.
7. Zwart PH, et al. (2008) Automated structure solution with the PHENIX suite. *Methods Mol Biol* 426:419–435.
8. Emsley P, Lohkamp B, Scott WG, Cowtan K (2010) Features and development of Coot. *Acta Crystallogr D Biol Crystallogr* 66(Pt 4):486–501.
9. Adams PD, et al. (2010) PHENIX: A comprehensive Python-based system for macromolecular structure solution. *Acta Crystallogr D Biol Crystallogr* 66(Pt 2):213–221.
10. Chen VB, et al. (2010) MolProbity: All-atom structure validation for macromolecular crystallography. *Acta Crystallogr D Biol Crystallogr* 66(Pt 1):12–21.
11. Berman HM, et al. (2000) The Protein Data Bank. *Nucleic Acids Res* 28(1):235–242.
12. Lovell SC, et al. (2003) Structure validation by Calpha geometry: Phi, psi and Cbeta deviation. *Proteins* 50(3):437–450.
13. Hura GL, et al. (2009) Robust, high-throughput solution structural analyses by small angle X-ray scattering (SAXS). *Nat Methods* 6(8):606–612.
14. Classen S, et al. (2013) Implementation and performance of SIBYLS: A dual endstation small-angle X-ray scattering and macromolecular crystallography beamline at the Advanced Light Source. *J Appl Cryst* 46(Pt 1):1–13.
15. Konarev PV, Volkov VV, Sokolova AV, Koch MHJ, Svergun DI (2003) PRIMUS: A Windows PC-based system for small-angle scattering data analysis. *J Appl Cryst* 36(5): 1277–1282.
16. Liu H, Hexemer A, Zwart PH (2012) The Small Angle Scattering ToolBox (SASTBX): An open-source software for biomolecular small-angle scattering. *J Appl Cryst* 45(3): 587–593.
17. Schneidman-Duhovny D, Hammel M, Sali A (2010) FoXS: A web server for rapid computation and fitting of SAXS profiles. *Nucleic Acids Res* 38(Web Server issue): W540-4.
18. Srivastava D, et al. (2010) Crystal structure of the bifunctional proline utilization A flavoenzyme from Bradyrhizobium japonicum. *Proc Natl Acad Sci USA* 107(7): 2878–2883.
19. Meek TD, Garvey EP, Santi DV (1985) Purification and characterization of the bifunctional thymidylate synthetase-dihydrofolate reductase from methotrexate-resistant Leishmania tropica. *Biochemistry* 24(3):678–686.
20. McNicholas S, Potterton E, Wilson KS, Noble ME (2011) Presenting your structures: The CCP4mg molecular-graphics software. *Acta Crystallogr D Biol Crystallogr* 67(Pt 4): 386–394.
21. Arnold K, Bordoli L, Kopp J, Schwede T (2006) The SWISS-MODEL workspace: A web-based environment for protein structure homology modelling. *Bioinformatics* 22(2): 195–201.
22. Thompson JD, Higgins DG, Gibson TJ (1994) CLUSTAL W: Improving the sensitivity of progressive multiple sequence alignment through sequence weighting, position-specific gap penalties and weight matrix choice. *Nucleic Acids Res* 22(22):4673–4680.
23. Gouet P, Robert X, Courcelle E (2003) ESPript/ENDscript: Extracting and rendering sequence and 3D information from atomic structures of proteins. *Nucleic Acids Res* 31(13):3320–3323.

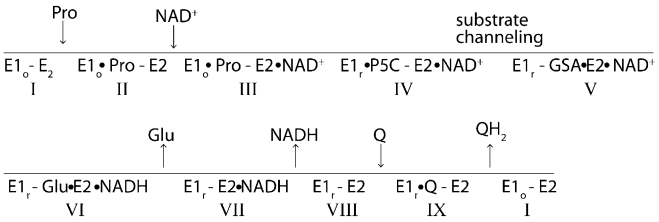

Fig. S1. General kinetic scheme for PutA. E1 and E2 refer to the PRODH and P5CDH active sites. The subscripts "o" and "r" denote the PRODH active site with the flavin in the oxidized and two-electron reduced states, respectively. Q and QH_2 denote the oxidized and reduced quinone.

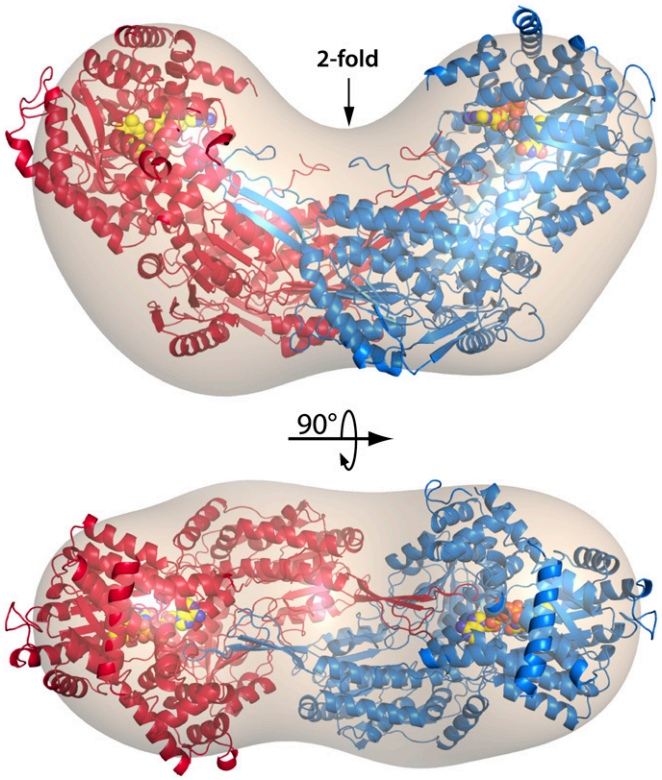

Fig. S2. Superposition of the SAXS shape reconstruction and the GsPutA dimer.

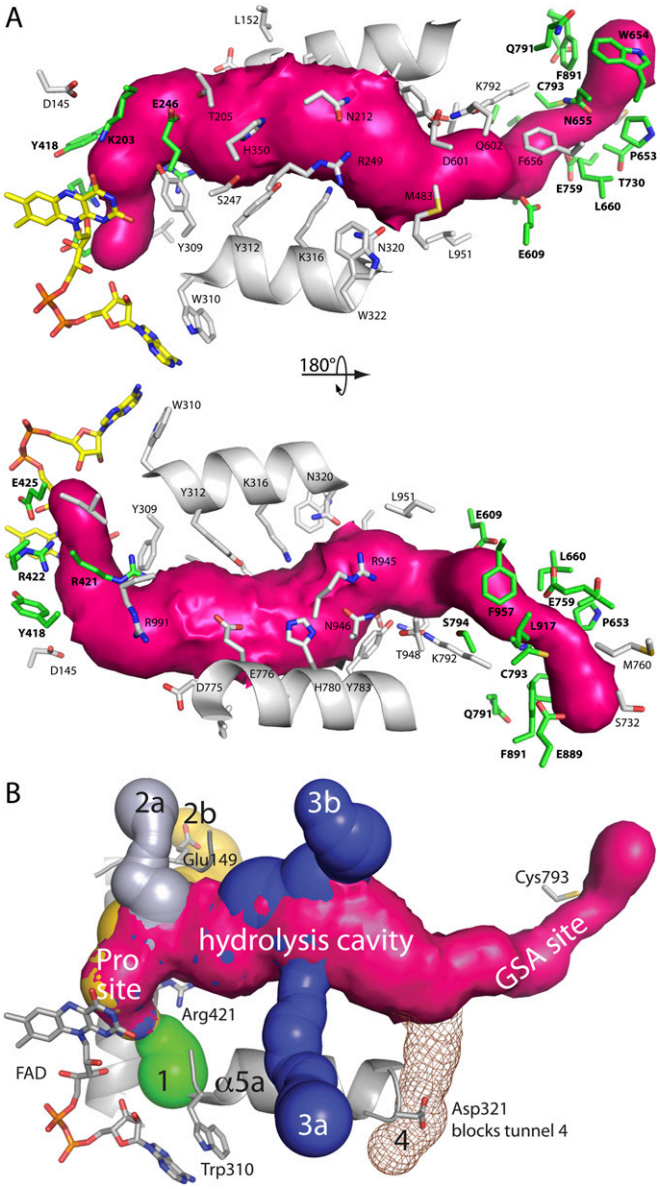

Fig. S3. Additional analysis of the tunnel system of GsPutA. (*A*) Two views of the main substrate-channeling tunnel of resting GsPutA, highlighting the composition of the walls of the tunnel. Residues that are identically conserved in PutA sequences are colored green with bold labels. (*B*) Surface rendering of the tunnel system of dithionite-reduced GsPutA. The brown mesh represents tunnel 4 in the resting enzyme. Asp321 blocks tunnel 4 in the reduced enzyme.

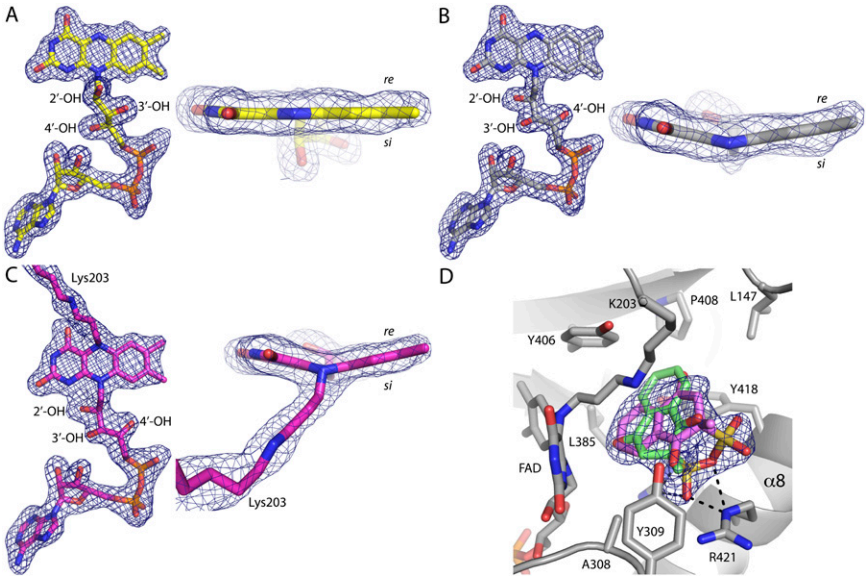

Fig. S4. Electron density maps. (*A*) The flavin of oxidized GsPutA. (*B*) The flavin of dithionite-reduced GsPutA. (*C*) The flavin of NPPG-inactivated GsPutA. The cages in *A*–*C* represent simulated annealing σ_A-weighted $F_o - F_c$ omit maps (3σ). (*D*) Electron density for the dual conformations of MB in protomer B of the asymmetric unit. The (*R*) enantiomer (green) has occupancy of 0.55 and is also present in the other GsPutA protomer (Fig. 4*C*). The (*S*) enantiomer (pink) has occupancy of 0.45. The cage represents a simulated annealing σ_A-weighted $F_o - F_c$ omit map (2.5σ).

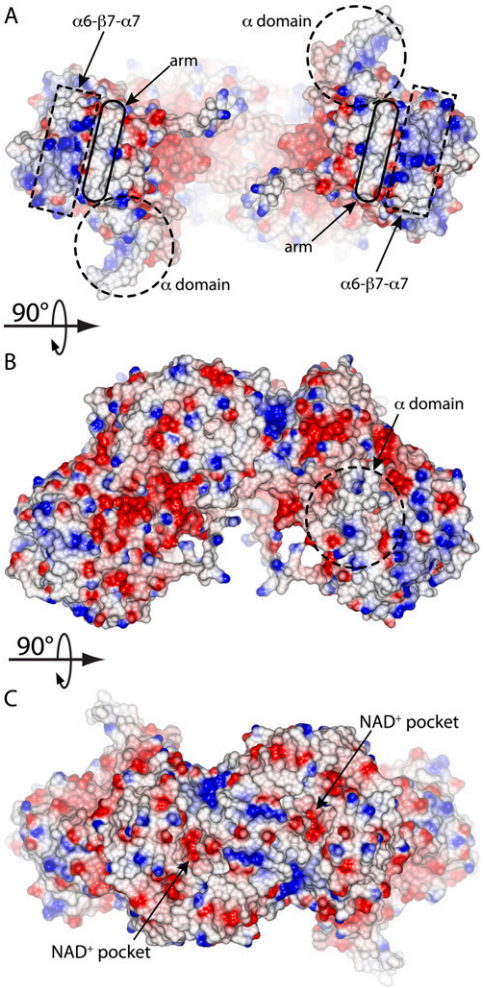

Fig. S5. Electrostatic potential surface of the GsPutA dimer. Three orthogonal views related by 90° rotations around the horizontal axis are shown. (*A*) The concave face viewed down the twofold axis. (*B*) The long side of the dimer. The twofold axis is vertical. (*C*) The convex face viewed down the twofold axis.

Table S1. Data collection and phasing statistics for GsPutA Hg derivative

Beamline	24-IDE
Wavelength, Å	0.97918
Space group	$P2_12_12_1$
Unit cell parameters, Å	
a	93.84
b	156.23
c	191.54
Resolution, Å	121.07–2.57
Observations	369,061
Unique reflections	90,248
$R_{merge}(I)$	0.105 (0.455)
$R_{meas}(I)$	0.149 (0.618)
$R_{pim}(I)$	0.072 (0.301)
Mean I/σ	12.2 (2.7)
Completeness, %	99.8 (99.2)
Multiplicity	4.1 (4.1)
Anomalous slope	1.16
No. of Hg sites	6
Figure of merit before DM	0.27
Figure of merit after DM	0.44
Auto-built model	
Total residues	1,762
Side chains placed	1,026
R_{cryst}	0.284
R_{free}	0.326

Values for the outer resolution shell of data are given in parentheses. DM, density modification.

Table S2. Data collection and refinement statistics for oxidized GsPutA structures

	Resting (I)	THFA (II)	L-lactate (II)	Zwittergent
Beamline	24-IDC	24-IDE	24-IDE	ALS 4.2.2
Space group	$P2_12_12_1$	$P2_12_12_1$	$P2_12_12_1$	$P2_12_12_1$
Unit cell parameters, Å				
a	95.25	95.62	95.65	94.08
b	151.21	151.74	152.06	152.21
c	175.13	176.21	175.13	190.76
Wavelength	0.97910	0.97918	0.97918	1.0000
Resolution, Å	49.05–1.90	48.62–2.10	175.13–2.20	47.04–1.90
Observations	898,584	489,887	563,664	1,166,275
Unique reflections	197,435	146,947	129,595	220,275
$R_{merge}(I)$	0.076 (0.536)	0.110 (0.605)	0.110 (0.716)	0.098 (0.683)
$R_{meas}(I)$	0.097 (0.703)	0.162 (0.823)	0.126 (0.832)	0.109 (0.777)
$R_{pim}(I)$	0.044 (0.325)	0.087 (0.452)	0.059 (0.413)	0.046 (0.366)
Mean I/σ	13.0 (2.2)	11.0 (2.2)	13.0 (2.4)	10.4 (2.0)
Completeness, %	99.1 (99.1)	98.5 (96.7)	99.5 (97.0)	99.4 (96.9)
Multiplicity	4.6 (4.5)	3.3 (3.2)	4.3 (3.8)	5.3 (4.3)
No. of protein residues	1,959	1,956	1,954	1,912
No. of atoms				
Protein	15,115	15,129	15,068	14,622
FAD	106	106	106	106
THFA	N/A	16	N/A	N/A
L-lactate	N/A	N/A	12	6
Zwittergent 3–12	N/A	N/A	N/A	9
MES	N/A	N/A	24	N/A
Water	1,208	738	629	1,122
Other	88	80	N/A	36
R_{cryst}	0.1626	0.1728	0.1798	0.1799
R_{free}	0.1924	0.2135	0.2200	0.2134
rmsd bond lengths, Å	0.007	0.007	0.008	0.008
rmsd bond angles, °	1.03	1.05	1.05	1.04
Ramachandran plot*				
Favored, %	98.20	98.46	98.30	97.89
Outliers, %	0.00	0.00	0.00	0.05
Average B, Å^2				
Protein	21.1	23.5	27.7	31.2
FAD	15.5	16.7	20.7	28.5
THFA	N/A	18.7	N/A	N/A
L-lactate	N/A	N/A	30.3	32.3
Zwittergent 3–12	N/A	N/A	N/A	44.8
MES	N/A	N/A	43.0	N/A
Water	25.9	25.6	27.1	29.0
Other	28.9	32.0	N/A	45.4
Coordinate error, Å†	0.19	0.25	0.26	0.20
PDB ID code	4NM9	4NMA	4NMB	4NMC

Values for the outer resolution shell of data are given in parentheses.
*The Ramachandran plot was generated with RAMPAGE via the PDB validation server.
†Maximum likelihood-based coordinate error estimate from phenix.refine.

Table S3. Data collection and refinement statistics for reduced/inactivated GsPutA structures

	Dithionite (VIII)	NPPG (VIII)	NPPG-MB (IX)
Beamline	24IDC	24IDE	24IDC
Space group	$P2_12_12_1$	$P2_12_12_1$	$P2_12_12_1$
Unit cell parameters, Å			
a	95.17	95.24	95.59
b	151.36	151.18	151.70
c	175.48	175.18	176.60
Wavelength	0.97910	0.97918	0.97910
Resolution, Å	49.09–1.98	175.18–2.09	47.60–1.95
Observations	651,971	654,722	691,229
Unique reflections	172,814	149,802	183,582
$R_{merge}(I)$	0.065 (0.605)	0.099 (0.531)	0.092 (0.858)
$R_{meas}(I)$	0.086 (0.748)	0.133 (0.719)	0.106 (0.997)
$R_{pim}(I)$	0.042 (0.369)	0.063 (0.347)	0.053 (0.498)
Mean I/σ	14.6 (2.4)	12.5 (2.5)	11.9 (1.8)
Completeness, %	98.2 (98.4)	97.1 (96.3)	98.5 (97.7)
Multiplicity	3.8 (3.8)	4.4 (4.2)	3.8 (3.8)
No. of protein residues	1,965	1,951	1,956
No. of atoms			
Protein	15,132	15,111	15,174
FAD	106	106	106
Modified Lys203	N/A	24	24
MB	N/A	N/A	51
Water	919	951	1,007
Other	56	64	32
R_{cryst}	0.1652	0.1691	0.1726
R_{free}	0.1988	0.2079	0.2026
rmsd bond lengths, Å	0.007	0.007	0.007
rmsd bond angles, °	1.03	1.03	1.06
Ramachandran plot*			
Favored, %	97.94	98.03	98.14
Outliers, %	0.00	0.00	0.10
Average B, $Å^2$			
Protein	24.5	24.6	21.6
FAD	19.6	19.4	16.5
Modified Lys203	NA	21.8	20.6
MB	NA	NA	31.5
Water	26.4	26.5	24.3
Other	29.3	29.0	26.5
Coordinate error, Å†	0.20	0.22	0.20
PDB code	4NMD	4NME	4NMF

Values for the outer resolution shell of data are given in parenthesis.
*The Ramachandran plot was generated with RAMPAGE via the PDB validation server.
†Maximum likelihood-based coordinate error estimate from phenix.refine.

Table S4. Steady-state kinetic parameters of GsPutA PRODH activity

Variable substrate	Fixed substrate	K_m	k_{cat}, s^{-1}	k_{cat}/K_m, $M^{-1}\cdot s^{-1}$
Menadione bisulfite	Proline*	10.5 ± 1.2 μM	0.66 ± 0.02	63,000 ± 7,000
Menadione	Proline*	8.2 ± 0.9 μM	0.97 ± 0.02	118,000 ± 13,000
Proline	Menadione bisulfite†	63 ± 8 mM	0.85 ± 0.03	13 ± 2
Proline	Menadione‡	89 ± 13 mM	0.67 ± 0.03	7 ± 1

*Fixed proline concentration of 350 mM.
†Fixed menadione bisulfite concentration of 150 μM.
‡Fixed menadione concentration of 100 μM.